European Journal of Nuclear Medicine and Molecular Imaging

Supplementary Materials for

Early prediction of lung lesion progression in COVID-19 patients with extended CT ventilation imaging

Cheng Wang[1,2,#], Lu Huang[3,#], Sa Xiao[2,#], Zimeng Li[2], Chaohui Ye[1,2], Liming Xia[3,*], Xin Zhou[2,*]

[1] School of Physics, Huazhong University of Science and Technology, Wuhan 430074, China

[2] State Key Laboratory of Magnetic Resonance and Atomic and Molecular Physics, National Center for Magnetic Resonance in Wuhan, Wuhan Institute of Physics and Mathematics, Innovation Academy for Precision Measurement Science and Technology, Chinese Academy of Sciences - Wuhan National Laboratory for Optoelectronics, Wuhan 430071, China

[3] Department of Radiology, Tongji Hospital, Tongji Medical College, Huazhong University of Science and Technology, Wuhan 430030, China

[#] These authors contributed equally to this work

* Corresponding author: Xin Zhou (xinzhou@wipm.ac.cn); Liming Xia (lmxia@tjh.tjmu.edu.cn)

This PDF file includes two parts:

Validation of CT-based ventilation

The relative change of lung volumes of interest region (e.g., left lung, right lung) between two CT scans is commonly used for verifying the accuracy of CT-based ventilation map [1, 2]. Therefore, we used the same way to evaluate the accuracy of the calculated CT-based ventilation. The consecutive healthy lung slices in CT1 and CT2 images of COVID-19 patients were selected. To make sure these slices could compose 3D subsets images, the number of consecutive slices was required above 10. Twelve patients satisfied this requirement. Then we measured the relative changes of lung volumes between the CT1 and CT2 subsets images to indicate the actual ventilation, as shown in Fig. S1a. We also calculated the mean FV values of these CT images. The mean ± SD of the measured relative changes and the calculated mean FV values were 0.11 ± 0.07 and 0.10 ± 0.06, and there was no significant difference between them (P = 0.247).

Fig. S1b displayed the Pearson correlation analysis between the measured relative changes and the calculated mean FV values. There was a high degree of correlation between the measured and calculated results (R = 0.945), which was comparable with the reported correlations in conventional CTVI method (R = 0.985 in Ref. [1] and R = 0.946 in Ref. [2]). Fig. S1c showed the Bland-Altman plot of the measured relative changes and the calculated mean FV values. The mean bias ± SD was 0.008 ± 0.022 (95% limit of agreement: –0.036 to 0.052). These results indicated that the measured relative changes of lung volumes and the calculated mean FV values were in good agreement. All these findings supported the accuracy of our method.

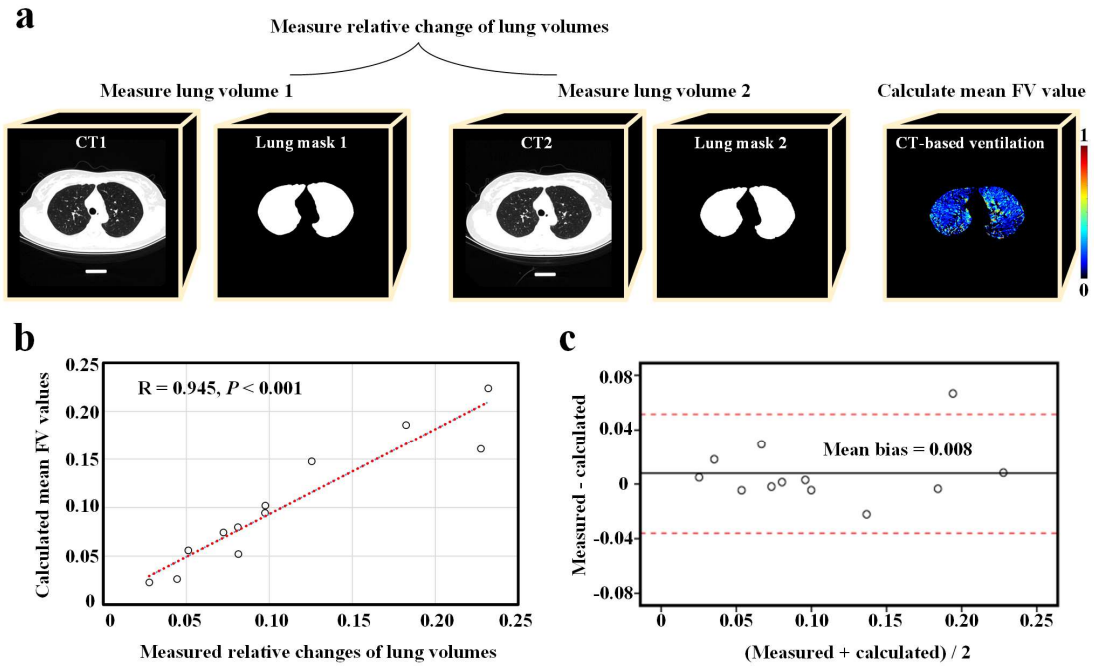

Fig. S1 The validation of CT-based ventilation. **a** The measurement of relative change of lung volumes. The CT1 and CT2 represented the first and second CT scans. **b** The correlation analysis results between the measured relative changes of lung volumes and the calculated mean FV values. **c** Bland-Altman plot of the measured relative changes of lung volumes and the calculated mean FV values

Evaluation of FV in visible lesions

To further evaluate the regional function and tissue property changes in the existed lesions due to the progression of COVID-19 pneumonia, the FV values and corresponding prediction map of visible lesions in CT2 image were also calculated. Fig. S2 showed the CT1 scan, CT2 scan, CT3 scan, and the prediction maps of visible lesions in CT2 for the three representative COVID-19 patients in Fig. 5. The results could be divided into two situations. In the first situation (the first patient in Fig. S1), the prediction map of visible lesions was composed of black (hypointense FV values), yellow (hyperintense FV values), and blue (normal FV values). Interestingly, the blue color areas were corresponded to the regional absorption of the visible lesions on CT2 (indicated by red cycles). This situation was rarely observed in this work. In 27 patients who had lesions on the CT2 image, only 5 patients (18.5%) had some regional normal FV values in visible lesions. In the second situation (the second and third patients in Fig. S2), the prediction map of visible lesions was only composed of black (hypointense FV values) and yellow (hyperintense FV values). This situation was commonly observed in the patients (81.5%). These findings suggested that the FV values of visible lesions in most patients were abnormal, which were consistent with the FV values of new lesions. Besides, only 5 patients had some regional normal FV values in the visible lesions, which may relate to the recovery of the disease. In this study, we focused on the prediction of new lesions in the early stage of COVID-19 disease. Whether the CTVI method could be used to evaluate the absorption of lung lesions in COVID-19 patients was beyond the scope of this work and could be explored in future studies.

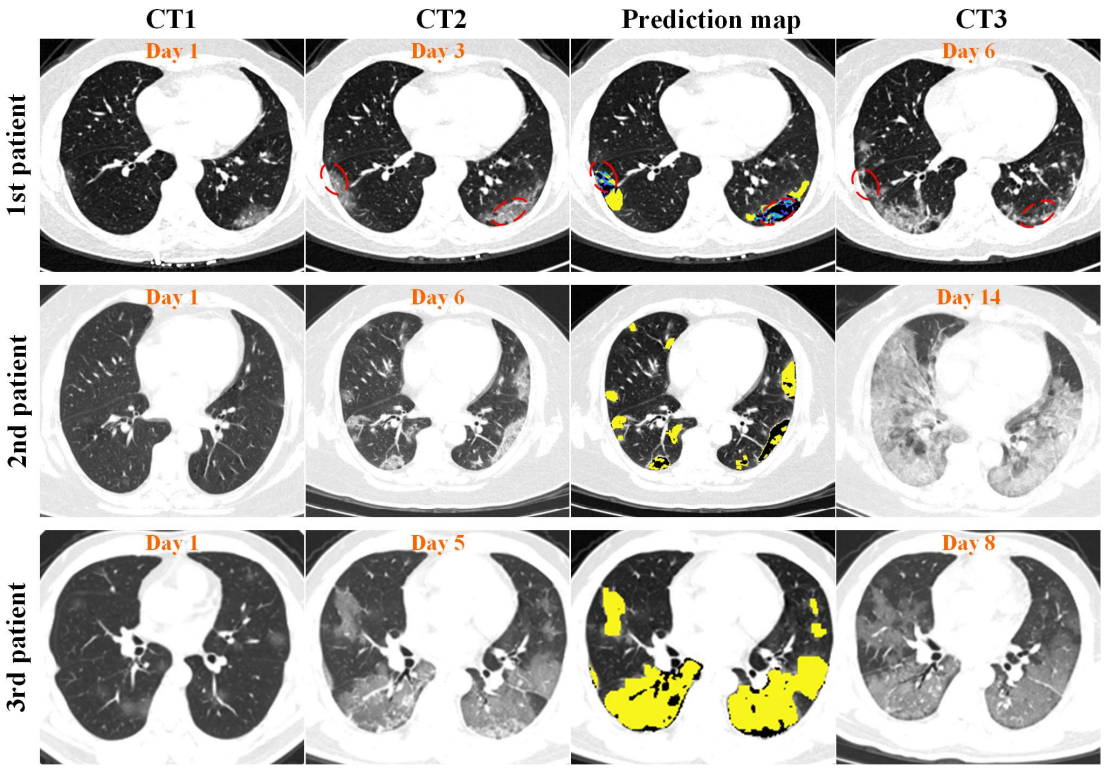

Fig. S2 CT1 scan, CT2 scan, CT3 scan, and the prediction maps of visible lesions in CT2 for the three representative COVID-19 patients in Fig. 5. The CT1 and CT2 scans represented the first two CT scans and were used to generate the FV values and corresponding prediction map. The CT3 scan represented the third CT scan and was used to validate the predicted results. For the first patient, the prediction map of visible lesions was composed of black (hypointense FV values), yellow (hyperintense FV values), and blue (normal FV values). The red cycles indicated the possible regional absorption of the visible lesions. For the second and third patients, the prediction map of visible lesions was only composed of black (hypointense FV values) and yellow (hyperintense FV values), which was consistent with the FV values of new lesions

References

1. Guerrero T, Sanders K, Noyola-Martinez J, et al. Quantification of regional ventilation from treatment planning CT. Int J Radiat Oncol. 2005;62(3):630-634.

2. Guerrero T, Sanders K, Castillo E, et al. Dynamic ventilation imaging from four-dimensional computed tomography. Phys Med Biol. 2006;51(4):777-791.